

Rainfall as a Driver for Near-Surface Turbulence and Air-Water Gas Exchange in Aquatic Systems

Eliana Bohórquez-Bedoya^{1,2,*}, Lorenzo Rovelli², and Andreas Lorke²

¹ Department of Geosciences and Environment, Universidad Nacional de Colombia, Medellín, Colombia.

² Institute for Environmental Sciences, University of Koblenz-Landau, Landau, Germany.

* Corresponding author: Eliana Bohórquez-Bedoya (elibohorquezbed@unal.edu.co)

Contents of this file

Figures S1 to S9

Additional Supporting Information (Files uploaded separately)

None

Introduction

The supporting information provided here consists of images showing the experimental setup and figures with specific results. The figures of the results were processed in Matlab R2021a. No anomalies are presented in the data.

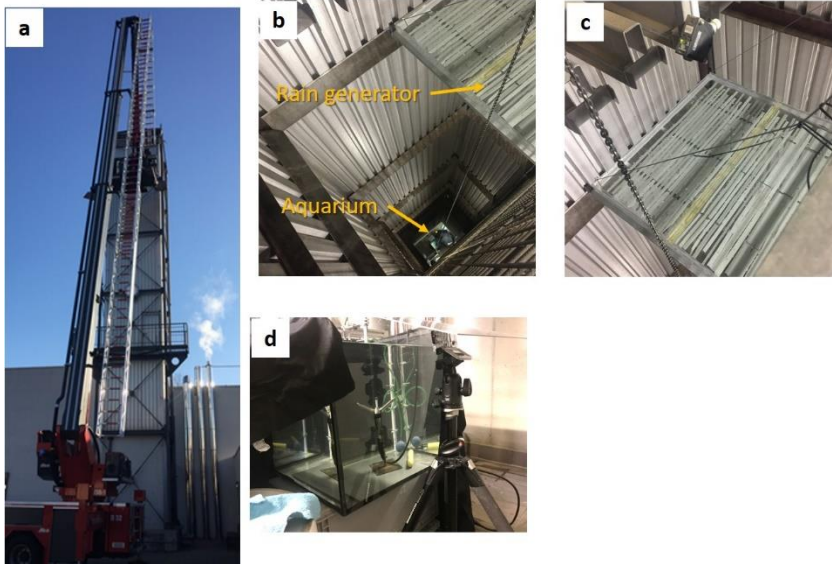


Figure S1. Pictures of the experimental setup: a) Hose-drying tower (approximately 20 m tall) of the municipal fire brigade in Landau, Germany, in which experiments were conducted. b) Inside view showing the rain generator in the top and the aquarium at the base of the tower. c) detailed view of the rain generator (cf. Fig. 1). d) Aquarium with sensors and camera mounting frame.



Figure S2. Picture of the rain generator: The outer aluminum frame (1 x 1 x 0.05 m) was filled with water and raindrops formed at regularly arranged holes in the transparent bottom plate. The rainfall rate was varied by closing or opening a varying number of holes using adhesive tape (visible as black and silver tape stripes in the picture).

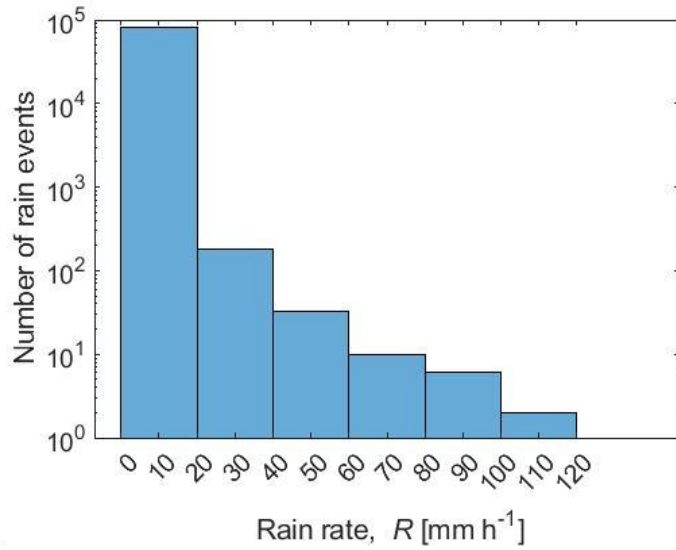


Figure S3. Histogram of local precipitation at Porce III reservoir, Colombia ($6^{\circ}54'12.6''N$, $75^{\circ}10'16.1''W$). Data were obtained from measurements with 1h resolution for the period between 1 January 2017 and 1 May 2019 ($n = 81601$).

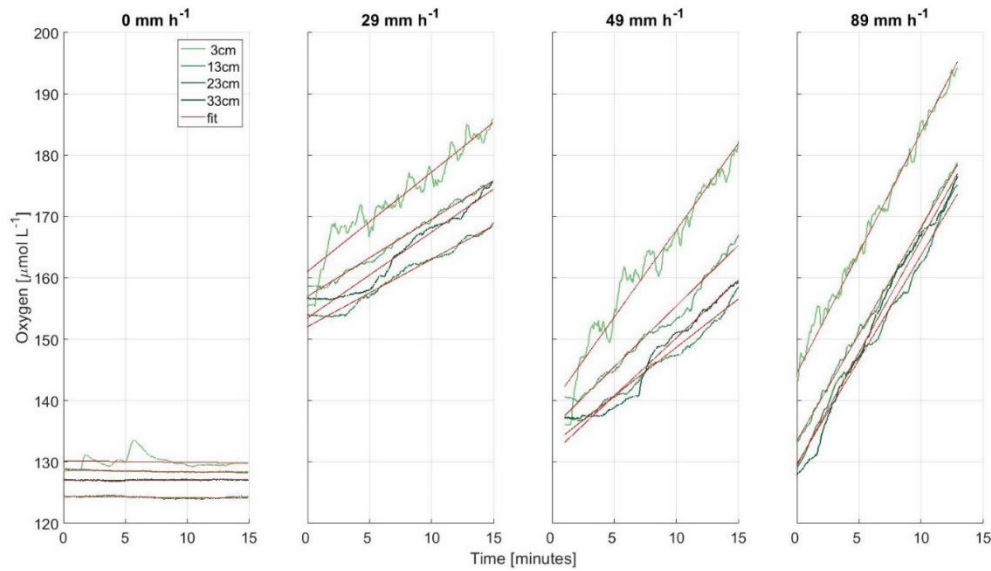


Figure S4. Time series of dissolved oxygen concentration at different sampling depth in the aquarium (line color, see legend) observed without rain and for three different rain rates (see panel headings). Red solid lines show linear regressions that were used for estimating the gas transfer velocity according to Eq. (3).

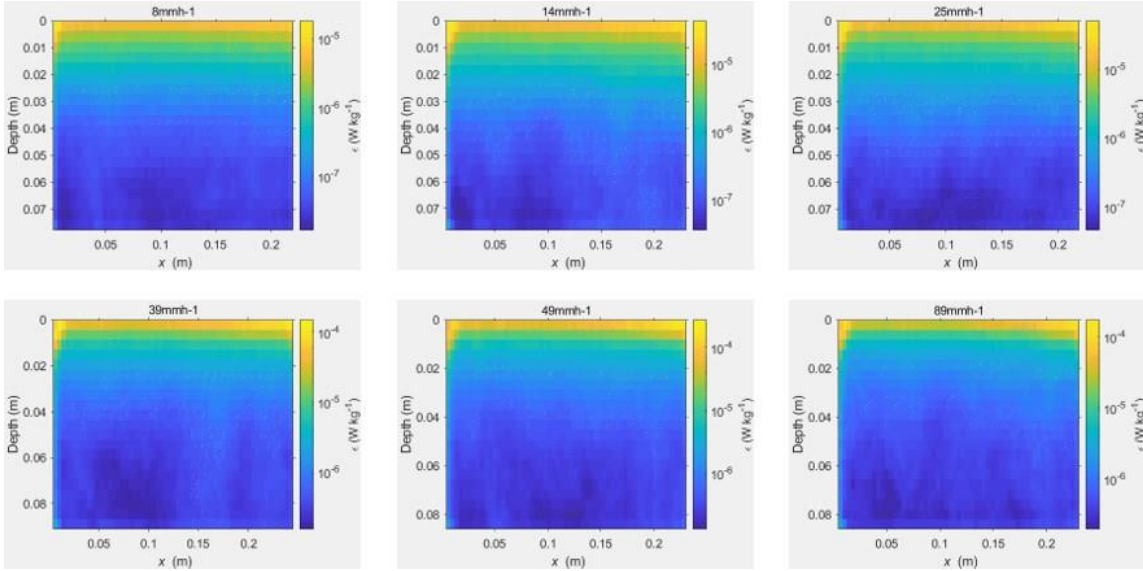


Figure S5. Spatial distribution of the time-averaged turbulent dissipation rates (ϵ_{t_avg}) for six different rain rates (see panel titles).

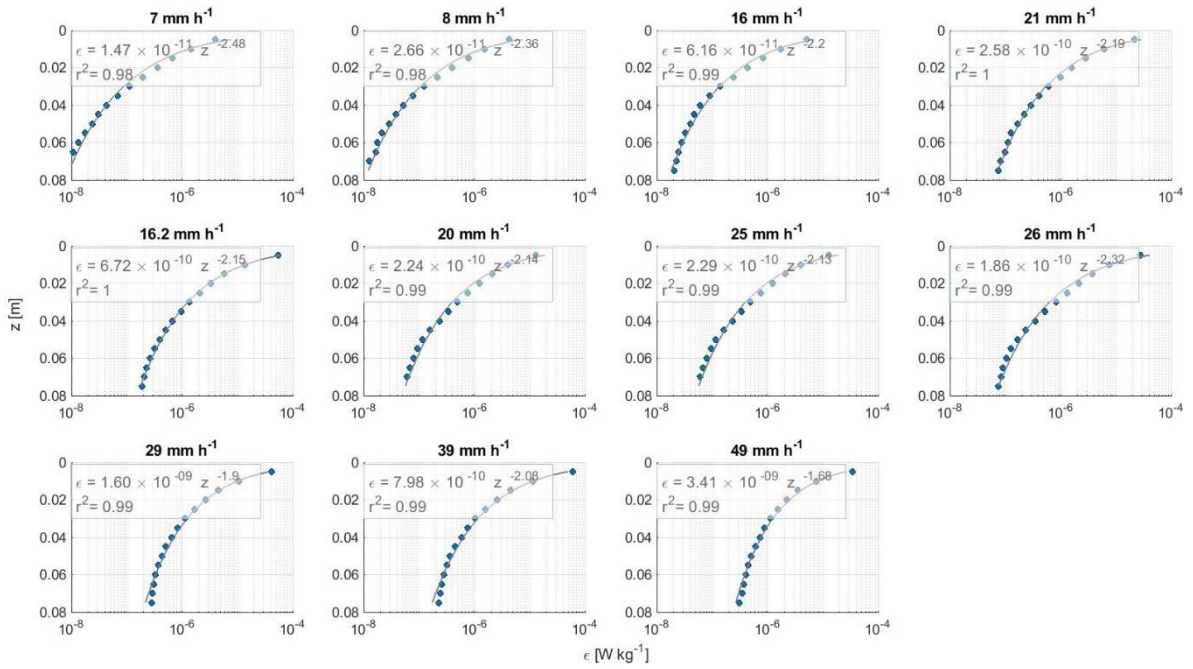


Figure S6. Mean vertical profiles of dissipation rates of turbulent kinetic energy for all measured rain rates (filled symbols). The solid lines show power-law fits according to the function shown in each legend.

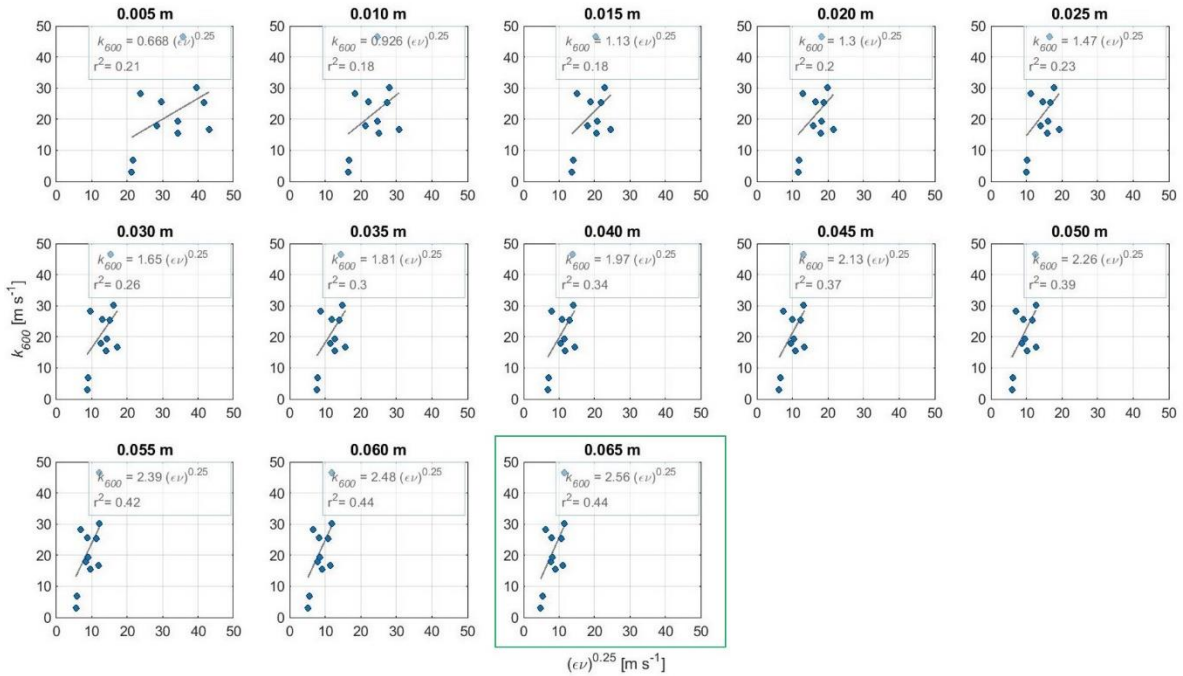


Figure S7. Normalized gas transfer velocities k_{600} versus the surface renewal model (Eq. (13)) for different water depth at which dissipation rates (ϵ) were measured. Solid lines show linear regressions according to the equation shown in the legends. The best fit, which was chosen to estimate the empirical coefficient A is highlighted by the green bounding box.

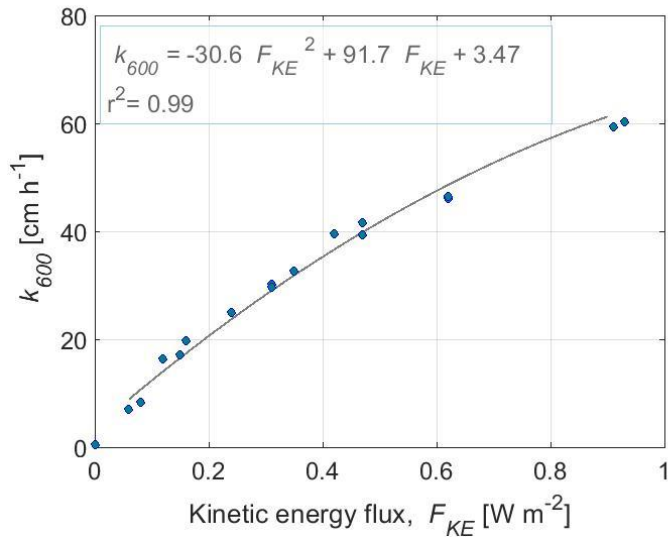


Figure S8. Normalized gas transfer velocity k_{600} as a function of the kinetic energy flux of rain reported in Ho et al. (1997) (their Table 1). The solid line shows a polynomial fit according the equation shown in the legend.

